3D printed PLGA implants: APF DDM vs. FDM

C. Bassand, L. Benabed, Sébastien Charlon, J. Verin, J. Freitag, F. Siepmann, J. Soulestin, J. Siepmann

Research article

3D Printed PLGA implants: APF DDM vs. FDM

C. Bassand[1°], L. Benabed[1°], S. Charlon[2], J. Verin[1], J. Freitag[1], F. Siepmann[1], J. Soulestin[2], J. Siepmann[1]*

[1]*Univ. Lille, Inserm, CHU Lille, U1008, F-59000 Lille, France*
[2]*IMT Lille Douai, École Nationale Supérieure Mines-Télécom Lille Douai, Materials & Processes Center, Cité Scientifique, Villeneuve d'Ascq Cedex, France*

[°]Authors contributed equally

*correspondence:
Prof. Dr. Juergen Siepmann
University of Lille, College of Pharmacy, INSERM U1008
3, rue du Professeur Laguesse, 59000 Lille, France
juergen.siepmann@univ-lille.fr

Abstract 3D Printing offers a considerable potential for personalized medicines. This is especially true for *customized* biodegradable implants, matching the specific needs of each patient. Poly(lactic-co-glycolic acid) (PLGA) is frequently used as matrix former in biodegradable implants. However, yet relatively little is known on the technologies, which can be used for the 3D printing of PLGA implants. The aim of this study was to compare: (i) Arburg Plastic Freeforming Droplet Deposition Modeling (APF DDM), and (ii) Fused Deposition Modeling (FDM) to print mesh-shaped, ibuprofen-loaded PLGA implants. During APF DDM, individual drug-polymer droplets are deposited, fusing together to form filaments, which build up the implants. During FDM, continuous drug-polymer filaments are deposited to form the meshes. The implants were thoroughly characterized before and after exposure to phosphate buffer pH 7.4 using optical and scanning electron microscopy, GPC, DSC, drug release measurements and monitoring dynamic changes in the systems' dry & wet mass and pH of the bulk fluid. Interestingly, the mesh structures were significantly differed, although the device design (composition & theoretical geometry) were the same. This could be explained by the fact that the deposition of individual droplets during APF DDM led to *curved and rather thick* filaments, resulting in a much lower mesh porosity. In contrast, FDM printing generated *straight and thinner* filaments: The open spaces between them were much larger and allowed convective mass transport during drug release. Consequently, most of the drug was already released after 4 d, when substantial PLGA set on. In the case of APF DDM printed implants, most of the drug was still entrapped at that time point and substantial polymer swelling transformed the meshes into more or less continuous PLGA gels. Hence, the diffusion pathways became much longer and ibuprofen release was controlled over 2 weeks.

Key words: PLGA; 3D printing; APF Droplet Deposition Modeling; Fused Deposition Modeling; ibuprofen

1. Introduction

Biodegradable controlled release implants offer a great potential to improve the therapeutic efficacy and minimize the risk of undesired side effects for a variety of drug treatments [1,2,3]. Poly (D,L lactic-co-glycolic acid) (PLGA) is frequently used as matrix former, trapping the drug and controlling its release rate [e.g., 4,5,6]. The key advantages of this polymer include: (i) it's good biocompatibility [7], (ii) complete degradation into lactic and glycolic acid, and (iii) the possibility to control drug release during very flexible release periods. Different manufacturing procedures can be used to prepare PLGA-based controlled release implants, including hot melt extrusion [8,9,10], compression [11], solvent-based techniques [12,13,14], and 3D printing [15].

3D Printing is a relatively new manufacturing technology in the pharmaceutical field [16,17,18,19,20,21]. One of its key advantages is that it offers the potential to *personalize* the drug product to the specific needs of each patient, e.g. for bone regeneration, cardio-vascular diseases, the treatment of pain, inflammation and/or infections [22,23,24,25,26]. For instance, 3D printers might be located in hospital pharmacies to manufacture on demand customized implants: Appropriate imaging technologies could be used to determine the specific geometry and size of the implant to fit the individual patient's anatomy. A variety of 3D printing technologies has been proposed, including Fused Deposition Modeling (FDM) [27,28], Droplet Deposition Modeling (DDM) [29], direct powder extrusion 3D printing [30], Powder Bed Fusion (PBF) [31], and Selective Laser Sintering (SLS) [32].

Yet, relatively little is known on the technologies, which can be used to 3D print biodegradable controlled release implants based on the polymer PLGA [33]. The most frequently used polymer in this field is poly (lactic acid) (PLA), and very often Fused Deposition Modeling (FDM) is applied [e.g., 34,35]. For FDM, generally, drug-loaded polymer filaments are prepared by hot melt extrusion in a first step. These filaments are then fed into the FDM printer, which heats the *filament* and deposits it on a plate to build up the implant in the desired geometry: layer by layer. In contrast, during Droplet Deposition Modelling (DDM), *individual droplets* are deposited on a plate. The droplets fuse together to form the implant. The viscosity of the liquid is key for droplet formation, so for many polymers high temperatures and pressures must be applied. The Arburg Plastic Freeforming (APF) technology [36,37] allows printing at temperatures above 300 °C and pressures above 400 bar. Wlesh et al. applied this APF DDM technology to print dapivirine-loaded, polyurethane-based vaginal rings [38]. Compared to FDM, the APF DDM technology does not require the preparation of drug loaded filaments with a sufficiently homogeneous diameter and appropriate mechanical properties as intermediate products.

The release mechanisms from PLGA-based drug delivery systems can be rather complex, because a variety of physico-chemical and biological processes can be involved [39,40,41]. This includes for example: water penetration into the system, drug dissolution, drug diffusion, polymer degradation, changes in the internal and external porosity of the device [42], local drops in micro-pH [43,44], autocatalytic effects, polymer swelling, osmotic effects [45], plasticizing effects of drugs and water for PLGA [46,47], diffusion of water-soluble degradation products, and limited solubility effects [48]. Often, polymer swelling is neglected, although this phenomenon has been shown to be of crucial importance in a variety of systems. For example, Bode et al. [49] demonstrated that it plays an "orchestrating role" in hot melt extruded PLGA implants loaded with dexamethasone. Upon contact with aqueous fluids, water penetrates into the system and the entire device is rather rapidly wetted. Thus, hydrolytic ester bond cleavage takes place throughout the implant ("bulk erosion"). However, since most PLGAs are hydrophobic, the amounts of water diffusing into the implant are limited. Importantly, each hydrolytic ester bond cleavage creates two new *hydrophilic* groups: an -OH and a -COOH group. Consequently, the system becomes more and more hydrophilic upon

degradation. Also, the average polymer molecular weight decreases, resulting in decreased macromolecular chain entanglement and less mechanical resistance to the penetration of large amounts of water. Furthermore, the generated water-soluble PLGA degradation products create a steadily increasing osmotic pressure inside the implants. After a certain lag phase (which depends on the type of PLGA: in particular its polymer molecular weight and type of end groups), substantial implant swelling sets on. The initially solid implant is transformed into a highly swollen PLGA gel. This has important consequences for the release of drug which still remains within the device at this time point: Potentially non-dissolved drug particles can dissolve in the large amounts of water, and the mobility of dissolved drug molecules/ions substantially increases. This results in a marked increase in the drug release rate, leading to complete drug exhaust: a final, rapid drug release phase is observed. In vitro, the substantial polymer swelling can be hindered/delayed by the presence of a surrounding gel (mimicking human tissue) [50,51]. Due to the complexity of the underlying drug release mechanisms in PLGA-based implants, device optimization is often cumbersome. When varying certain formulation or processing parameters, sometimes surprising tendencies can be observed. A better understanding of how drug release is controlled from this type of advanced delivery systems can very much facilitate and accelerate research and product development in this field.

The aim of this study was to prepare PLGA-based implants using 2 different 3D printing technologies: APF DDM and FDM. Ibuprofen was used as a low molecular weight, acidic model drug. But since ibuprofen is an anti-inflammatory drug, the printed biodegradable implants can also have therapeutic applications. 3 Dimensional meshes were printed with the same composition and identical (theoretical) design (geometry and size). Drug release was measured in phosphate buffer pH 7.4 at 37 °C. Optical and scanning electron microscopy, GPC, DSC, and gravimetric monitoring of dynamic changes in the systems' dry & wet mass as well as pH measurements of the bulk fluid were performed to better understand the underlying drug release mechanisms.

2. Materials and methods

2.1. Materials

Poly (D,L lactic-co-glycolic acid) (PLGA, 50:50 lactic acid: glycolic acid; Resomer RG 503H; Evonik, Darmstadt, Germany); ibuprofen (BASF, Ludwigshafen, Germany); agarose (genetic analysis grade) and tetrahydrofuran (HPLC grade) (Fisher Scientific, Illkirch, France); potassium dihydrogen orthophosphate and sodium hydroxide (Acros Organics, Geel, Belgium); acetonitrile (VWR, Fontenoy-sous-Bois, France); sodium hydrogen phosphate (Na_2HPO_4; Panreac Quimica, Barcelona, Spain).

2.2. Implant printing: APF DDM

PLGA was milled with a grinder (4 x 30 s; Valentin; Seb, Ecully, France). Appropriate amounts of polymer and drug powders (ibuprofen was used as received) were manually blended for 5 min with a mortar and a pestle, followed by extrusion using a Nano 16 twin-screw extruder (screw diameter = 16 mm, length/diameter ratio = 26.25, gravitational feeder; Leistritz, Nuremberg, Germany), equipped with a 2 mm diameter die. The process temperatures were kept constant at 80 - 75 - 70 - 65 °C (die - zone 3 - zone 2 - zone 1). The screw speed was set at 50 rpm, the screw configuration is illustrated in Figure S1. After cooling, the hot melt extrudates were manually cut into cylinders of 5 mm length. In this article, these cylinders are also called "pellets". They served as intermediate product and were fed into the feeder of an Arburg Plastic Freeforming (APF) printer (Freeformer, Arburg, Germany), which was used to print ibuprofen-loaded PLGA implants in the form of parallelepiped-shaped meshes (10 x 10 x 2.5 mm). The applied processing parameters are given in Table 1.

Table 1*: Printing parameters used for the preparation of ibuprofen-loaded PLGA implants by APF DDM and FDM.*

	APF DDM	**FDM**
Number of contouring layers	0	
Number of lower and upper layers	0	
Filling pattern	ZigZag	
Filling density (%)	30	
Nozzle diameter (mm)	0.25	
Layer thickness (mm)	0.25	
Printing temperature (°C)	zone 1: 120 zone 2: 110 zone 3: 110	First layer: 125 Otherwise: 115
Printing speed (mm/s)	40	50
Plate temperature (°C)	25	30
Ventilation (%)	Not applicable	10
Speed of retraction (mm/s)	Not applicable	40

2.3. Implant printing: FDM

PLGA was milled with a grinder (4 x 30 s; Valentin). Appropriate amounts of polymer and ibuprofen powders (the drug was used as received) were manually blended for 5 min with a mortar and a pestle. The mixture was melted on a hot film applicator plate (110 °C, 6 min; Erichsen, Rueil-Malmaison, France), followed by hot melt extrusion as described in *section 2.2.*, except that: (i) a 4 mm die was used, (ii) the die temperature was set to 70 ° C, and (iii) a feeder flow regulator was used, operating at a speed of 5-8 mL/min. The diameter of the filament obtained at the exit of the extruder was controlled by a laser sensor (target diameter between 1.60 and 1.80 mm; Tollerance Puller Noztek, Shoreham-by-Sea, UK). The filaments served as intermediate product and were fed into a Volumic 30 Stream Ultra printer (Volumic, Nice, France), which was used to print ibuprofen-loaded PLGA implants in the form of parallelepiped-shaped meshes (10 x 10 x 2.5 mm). The applied processing parameters are given in Table 1.

2.4. Optical microscopy

Pictures of implants were taken using a SZN-6 trinocular stereo zoom microscope (Optika, Ponteranica, Italy), equipped with an optical camera (Optika Vison Lite 2.1 software). The lengths/width and mesh pore size were determined using the ImageJ software (US National Institutes of Health, Bethesda, Maryland, USA). Mean values +/- standard deviations are reported (n = 36 for APF DDM; n = 12 for FDM).

2.5. Implant thickness

The thickness of the implant meshes before exposure to the release medium was determined with a micrometer gauge (Digimatic Micrometer; Mitutoyo, Tokyo, Japan). Mean values +/- standard deviations are reported (n = 3).

2.6. Practical drug loading

Hot melt extruded pellets and pieces of 3D printed implants were accurately weighed and dissolved in 5 mL acetonitrile, followed by filtration (PVDF syringe filters, 0.45 µm; Agilent

Technologies, Santa Clara, USA). The drug concentrations of the obtained solutions were determined by HPLC-UV analysis using a Thermo Fisher Scientific Ultimate 3000 Series HPLC, equipped with a LPG 3400 SD/RS pump, an auto sampler (WPS-3000 SL) and a UV-Vis detector (VWD-3400RS) (Thermo Fisher Scientific, Waltham, USA). A reversed phase column C18 (Gemini 5 µm; 110 A°; 150 x 4.6 mm; Phenomenex, Le Pecq, France) was used. The mobile phase was a mixture of 30 mM Na_2HPO_4 pH 7.0: acetonitrile (60:40, v:v). The detection wavelength was 225 nm, and the flow rate 0.5 mL/min. Ten microliter samples were injected. Mean values +/- standard deviations are reported (n = 3).

2.7. Differential scanning calorimetry (DSC)

DSC thermograms of the raw materials (PLGA and ibuprofen), hot melt extruded pellets, filaments, and 3D printed implants were recorded using a DCS1 Star System (Mettler Toledo, Greifensee, Switzerland). Approximately 5 mg samples were heated in pierced aluminum pans as follows: from -70 to 120 °C, cooling to -70 °C, re-heating to 120 °C (heating/cooling rate = 10 °C/min). The reported glass temperatures (Tgs) were determined from the *1st heating cycles* in the case of the hot melt extruded pellets, filaments and 3D printed meshes (the thermal history being of interest), and from the *2nd heating cycle* in the case of raw material (the thermal history not being of interest). All experiments were conducted in triplicate. Mean values +/- standard deviations are reported.

2.8. Gel permeation chromatography (GPC)

The average polymer molecular weight (Mw) of the PLGA was determined by gel permeation chromatography (GPC) as follows: Samples of raw material, hot melt extruded pellets, filaments and 3D printed implants were dissolved in tetrahydrofuran (3 mg/mL). Fifty µL samples were injected into an Alliance GPC (refractometer detector: 2414 RI, separation module e2695, Empower GPC software; Waters, Milford, USA), equipped with a PLgel 5 µm MIXED-D column (kept at 35°C, 7.8 × 300 mm; Agilent). Tetrahydrofuran was the mobile phase (flow rate: 1 mL/min). Polystyrene standards with molecular weights between 1,480 and 70,950 Da (Polymer Laboratories, Varian, Les Ulis, France) were used to prepare the calibration curve. All experiments were conducted in triplicate. Mean values +/- standard deviations are reported.

2.9. In vitro drug release

3D printed PLGA implants were placed into 50 mL tubes (1 mesh per tube; Corning-Falcon, New York, USA), filled with 50 mL phosphate buffer pH 7.4 USP 42. The tubes were placed in a horizontal shaker (80 rpm, 37°C; GFL 3033; Gesellschaft fuer Labortechnik, Burgwedel, Germany). At predetermined time points, the entire bulk fluid was replaced by fresh release medium. The withdrawn samples were filtered (PVDF syringe filter, 0.45 µm; Agilent) and analyzed for their ibuprofen contents by HPLC-UV, as described in *section 2.6*. Throughout the experiments, sink conditions were provided in all cases.

Furthermore, at pre-determined time points, the pH of the release medium was measured using a pH meter (InoLab pH Level 1; WTW, Weilheim, Germany), and pictures of the PLGA meshes were taken as described in *section 2.4*.

All experiments were conducted in triplicate. Mean values +/- standard deviations are reported.

2.10. Implant swelling

PLGA meshes were treated as described in *section 2.9.* for the in vitro drug release measurements. At pre-determined time points, implant samples were withdrawn and excess water was carefully removed using Kimtech precision wipes (Kimberly-Clark, Rouen, France).

The meshes were weighed [*wet mass (t)*], and the *changes in wet mass (%) (t)* were calculated as follows:

$$change\ in\ wet\ mass\ (\%)(t) = \frac{wet\ mass\ (t) - mass\ (t=0)}{mass\ (t=0)} \times 100\ \% \quad (1)$$

where *mass (t = 0)* denotes the implant mass before exposure to the release medium.

All experiments were conducted in triplicate. Mean values +/- standard deviations are reported.

2.11. Implant erosion and PLGA degradation

PLGA meshes were treated as described in *section 2.9.* for the in vitro drug release measurements. At pre-determined time points, implant samples were withdrawn and freeze dried (freezing at -45°C for 2 h 35 min, primary drying at -20 °C/0.940 mbar for 35 h 10 min, secondary drying at +20 °C/0.0050 mbar for 35 h; Christ Alpha 2-4 LSC+; Martin Christ, Osterode, Germany). The dried meshes were weighed [*dry mass (t)*] and the implant's *dry mass (%) (t)* was calculated as follows:

$$dry\ mass\ (\%)(t) = \frac{dry\ mass\ (t)}{mass\ (t=0)} \times 100\ \% \quad (2)$$

where *mass (t = 0)* denotes the implant's mass before exposure to the release medium.

All experiments were conducted in triplicate. Mean values +/- standard deviations are reported.

The average polymer molecular weight (Mw) of the PLGA in the withdrawn samples was determined by gel permeation chromatography (GPC) as described in *section 2.8.*

2.12. Scanning Electron Microscopy (SEM)

The internal and external morphology of the implants before and after exposure to the release medium was studied using a JEOL Field Emission Scanning Electron Microscope (JSM-7800F, Japan) and the Aztec 3.3 software (Oxford Instruments, Oxfordshire, England). Samples were fixed with a ribbon carbon double-sided adhesive and covered with a fine chrome layer. In the case of implants, which had been exposed to the release medium, the meshes were treated as described for the in vitro release studies (*section 2.9*). At predetermined time points, implant samples were withdrawn, optionally cut using a scalpel (for cross-sections), and freeze-dried (as described in *section 2.11.*).

3. Results and discussion

3.1. Implant manufacturing

Figure 1 illustrates the applied 3D printing techniques which were used to prepare ibuprofen-loaded PLGA implants with the geometry of meshes: A) Arburg Plastic Freeforming Droplet Deposition Modeling (APF DDM), and B) Fused Deposition Modeling (FDM). In the case of APF DDM, the 3D printer was fed with ibuprofen-loaded PLGA "pellets". The latter were prepared by hot melt extrusion of a drug – polymer powder blend (15 % ibuprofen, 85 % PLGA), using a spherical die. The obtained filament was cut into small cylinders (2 mm diameter, 5 mm length) (called "pellets" in this article). The pellets were introduced into a barrel, which was heated to 110-120 °C, as illustrated in Figure 1A. In the screw, the pellets were plasticized by the generated shear. The molten mixture was transported and injected by the displacement of the screw into the nozzle (diameter 0.25 mm). At the nozzle, individual droplets were discharged, using a Piezo actuator. The droplets were deposited onto the building plate, which was kept at room temperature. Because of the high frequency used for opening and

closing of the nozzle (140 Hz), the formation of a continuous filament ("droplet string") was observed. This filament formed a mesh, as schematically illustrated at the top on the right hand side of Figure 2 (the 3D printer worked in "ZigZag" mode). The layer thickness was set to 0.25 mm, the filling density to 30 %: This means that, theoretically, 30 % of the printed mesh are solid drug-polymer filaments and 70 % are empty spaces ("holes"). However, as it can be seen in the macroscopic pictures at the top of Figure 2, the formed filaments were not straight, but curved, so that the *real* filling density was higher than 30%. The printing speed was set to 40 mm/s. The outer dimensions of the parallelepiped-shaped meshes were as follows: length = width = 10.4 +/- 0.2 mm, thickness = 2.5 +/- 0.0 mm (Table 2). The weight of a mesh-shaped implant was 212 +/- 8 mg. The practical drug loading was 13.8 +/- 0.1 %.

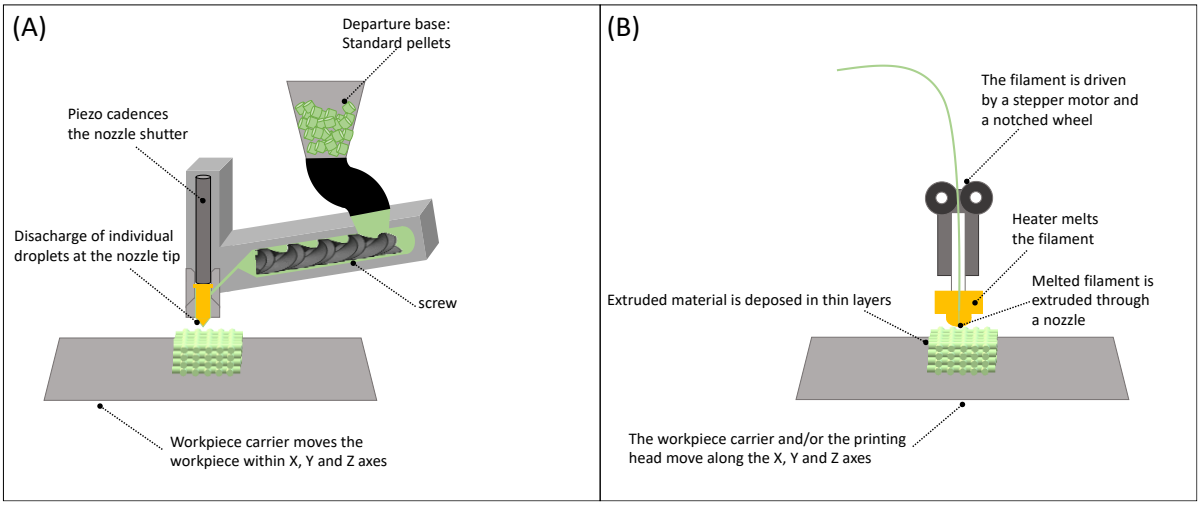

Fig 1: Schematic presentation of the investigated 3D printing techniques: (A) Arburg Plastic Freeforming Droplet Deposition Modeling (APF DDM), and (B) Fused Deposition Modeling (FDM).

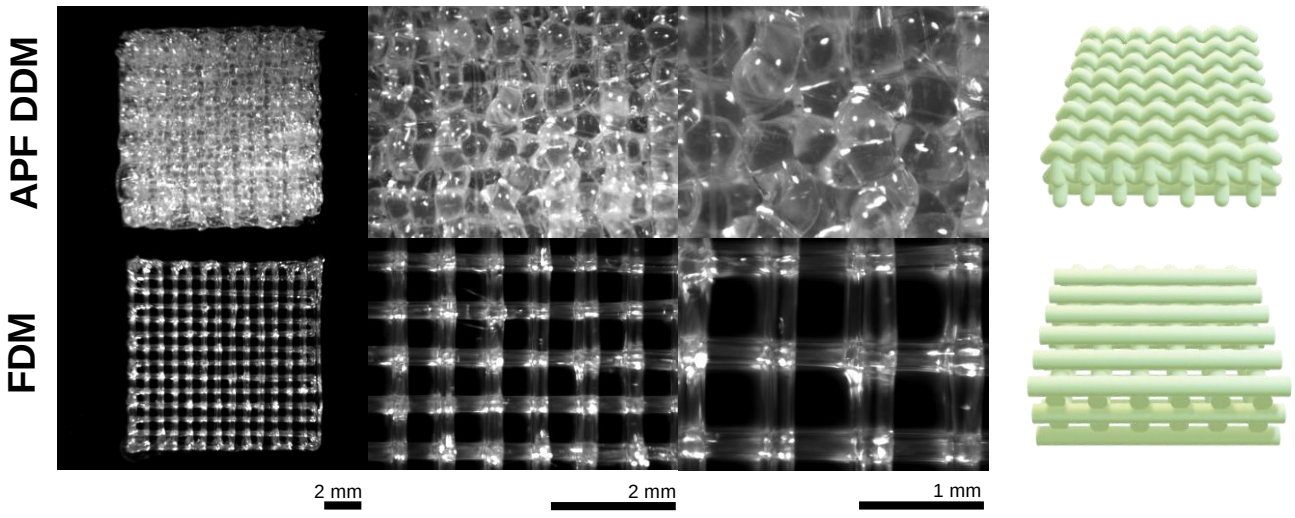

Fig 2: Optical macroscopy pictures of ibuprofen-loaded PLGA implants (meshes) prepared by Droplet Deposition Modeling (APF DDM) or Fused Deposition Modeling (FDM), before exposure to the release medium. The cartoons on the right hand side illustrate the real structures of the mesh-shaped implants.

***Table 2**: Key properties of the investigated PLGA implants before exposure to the release medium (Tg: glass transition temperature, Mw: molecular weight). Mean values ± standard deviations are indicated (n = 36 for weight, length, width and mesh pore size; n = 6 for practical drug loading; n = 3 for thickness, Tg, and Mw).*

	APF DDM	**FDM**
Weight (mg)	212.1 ± 8.4	89.7 ± 8.7
Length = width (mm)	10.4 ± 0.2	10.0 ± 0.1
Thickness (mm)	2.45 ± 0.04	2.50 ± 0.02
Mesh pore size (mm)	0.5 ± 0.1	0.5 ± 0.2
Practical drug loading (%)	13.8 ± 0.1	11.8 ± 0.2
Tg (°C)	34.6 ± 0.1	35.4 ± 0.3
Mw (kDa)	15.8 ± 0.3	19.6 ± 0.5

The manufacturing of mesh-shaped PLGA implants of the same composition (15 % ibuprofen, 85 % PLGA) prepared by FDM printing is illustrated in Figure 1B. The 3D printer was fed with an ibuprofen-loaded PLGA filament, which was prepared by hot melt extrusion. Please note that the processing conditions for the hot melt extrusion of these filaments were different from those applied for the preparation of the drug loaded pellets used for APF DDM printing: (i) a 2 mm die was used (vs. 4 mm), (ii) the die temperature was 70 ° C (vs. 80 °C), and (iii) a feeder flow regulator was used (operating at 5-8 mL/min). This was to assure that a filament with a diameter of 1.75 mm was obtained with limited thickness variations (this is critical for the feeding of the printer). During 3D printing, a heater melted the filament (Figure 1B), which was extruded through a nozzle. The filament was deposited on a plate, kept at 30 °C. As for APF DDM, the printer operated in "ZigZag" mode, the nozzle diameter was 0.25 mm and the design of the implant mesh was identical: layer thickness = 0.25 mm, theoretical filling density = 30 %. The printing temperature was 125 °C for the first layer, and 115 °C afterwards (the higher temperature for the first layer aims at improving the adhesion onto the plate). The ventilation was set to 10 % and the speed of retraction to 40 mm/s. Importantly, the filaments deposited by the FDM printer were straight, in contrast to the curved filaments created by the APF DDM printer under the selected processing conditions (Figure 2). In addition, the APF DDM printed filaments were thicker than the FDM printed filaments. Consequently, the *real* porosity of the FDM printed meshes was much higher compared to the porosity of the APF DDM printed implants. The weight of the investigated parallelepiped-shaped meshes (length = width = 10.0 +/- 0.1 mm, thickness = 2.5 +/- 0.0 mm) was 89.7 +/- 8.7 mg for FDM, compared to 212.1 +/- 8.4 mg for APF DDM. Thus, the fact that *discontinuous* flow through the nozzle occurrs during DDM, and *continuous* flow during FDM, can lead to major differences in key features of the implants, e.g. in the *real* filling density, as it was observed in this study. However, please note that different processing parameters used during

FDM and APF DDM printing can lead to differences in the resulting *real* mesh geometries. The practical drug loading of a FDM printed implant was 11.8 +/- 0.2 %. This was slightly lower than for the APF DDM printed meshes (13.8 +/- 0.1 %).

3.2. Physicochemical key properties

Figure 3 shows SEM pictures of surfaces and cross sections of implants printed by APF DDM and FDM at different degrees of magnification, before exposure to the release medium. As it can be seen, the surfaces of the ibuprofen-PLGA filaments were smooth and non-porous in both cases. The cross sections show a homogeneous inner filament structure, irrespective of the 3D printing technology. At higher magnification, numerous tiny pores become visible. This might be due to the exposure of the drug-polymer blends to high temperatures during manufacturing (> 100 °C, Table 1), leading to the evaporation of residual water and/or ibuprofen (which has a melting point of 79 °C).

The exposure to heat and shear forces during hot melt extrusion (to prepare the intermediate "pellets" and filaments) and subsequent 3D printing partially degraded the PLGA: As illustrated in Figure 4, the average polymer molecular weight (Mw) of the polyester decreased from 23 kDa in the raw material to 21 and 16 kDa in the hot melt extruded "pellets" and APF DDM printed implants, and to 21 and 20 kDa in the hot melt extruded filaments and FDM printed implants, respectively. PLGA is known to be degraded upon exposure to heat and high shear forces. The importance of the decrease in Mw observed in this study is consistent with the applied temperatures and pressures. For example, the polymer molecular weight was lowest in APF DDM printed meshes, for which temperatures up to 120 °C and pressures of more than 400 bar were applied during manufacturing. Please note that the differences in PLGA Mw between the hot melt extruded "pellets" used for APF DDM printing and the hot melt extruded filaments used for FDM printing were not very pronounced. Thus, the differences in the applied processing parameters for hot melt extrusion did not have a major impact on the degree of PLGA degradation.

Figure 5 shows the DSC thermograms of the investigated raw materials (PLGA and ibuprofen), intermediate products (ibuprofen-PLGA "pellets" and filaments), and 3D printed implants (prepared by APF DDM and FDM). The black flashes highlight the melting of crystalline ibuprofen. As it can be seen, glass transitions were observed in all intermediate products and implants. The respective glass transition temperatures (Tgs) were as follows: PLGA raw material: 47.2 +/ 0.1 °C, "pellets": 34.1 +/ 0.3 °C; filaments: : 33.7 +/ 0.6 °C, APF DDM printed implants: : 34.6 +/ 0.1 °C; FDM printed implants: : 35.4 +/ 0.3 °C. These results are in good agreement with: (i) the previously reported plasticizing activity of ibuprofen for PLGA [52], and (ii) the fact that at least 10% (w/w) of this drug can *dissolve* in this PLGA grade [52]. The elevated temperatures and shear forces during hot melt extrusion and 3D printing allowed the crystalline ibuprofen raw material to dissolve to a large extent within the polymer. The partially observed melting of minor amounts of ibuprofen crystals indicate that not all of the drug was always completely dissolved in the polymer. In FDM printed implants, no ibuprofen melting peak was visible in the DSC thermogram.

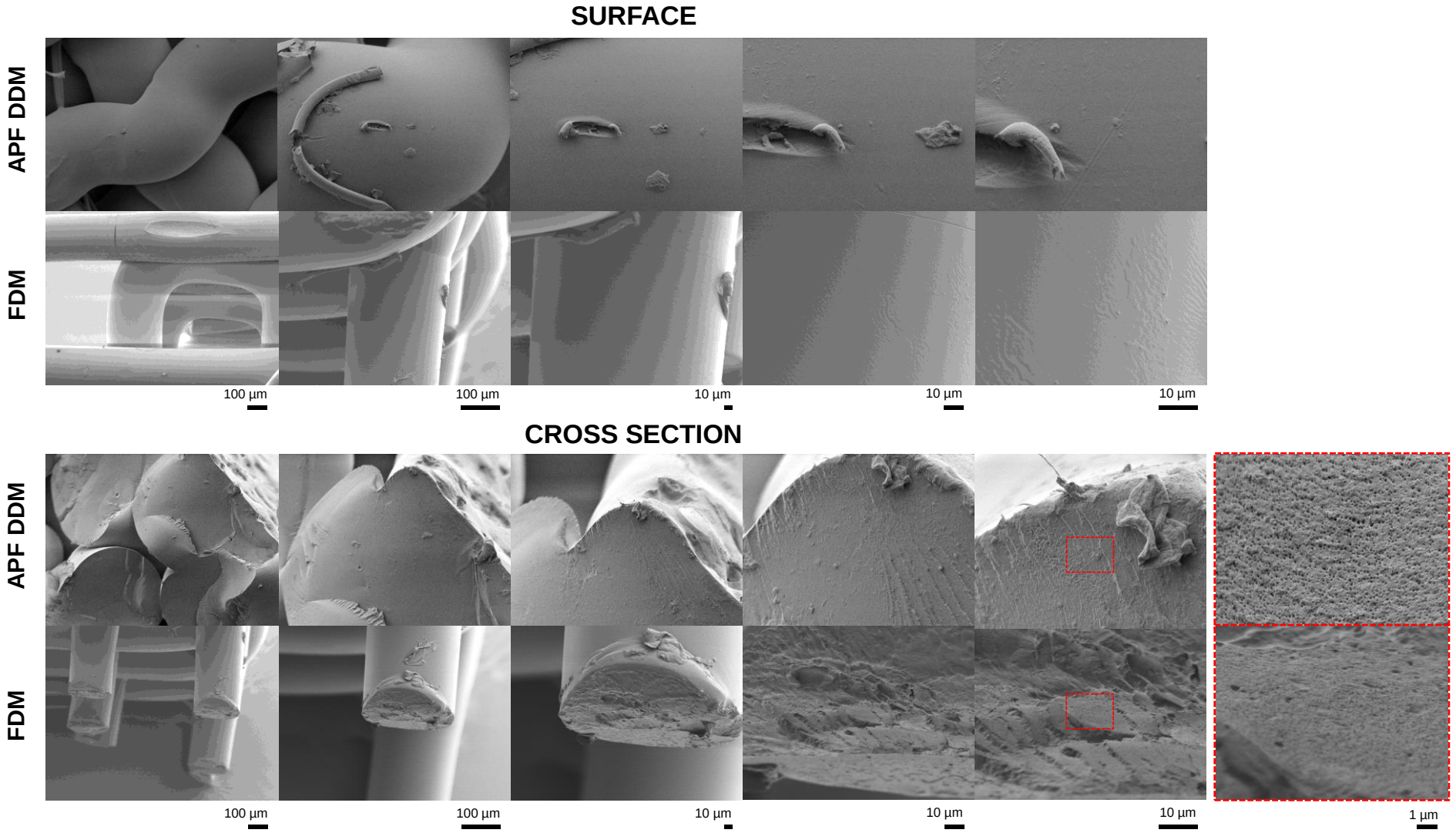

Fig 3: SEM pictures of surfaces and cross sections of ibuprofen-loaded PLGA meshes prepared by Droplet Deposition Modeling (APF DDM) or Fused Deposition Modeling (FDM), before exposure to the release medium. The red rectangles indicate specific regions observed at different degrees of magnification.

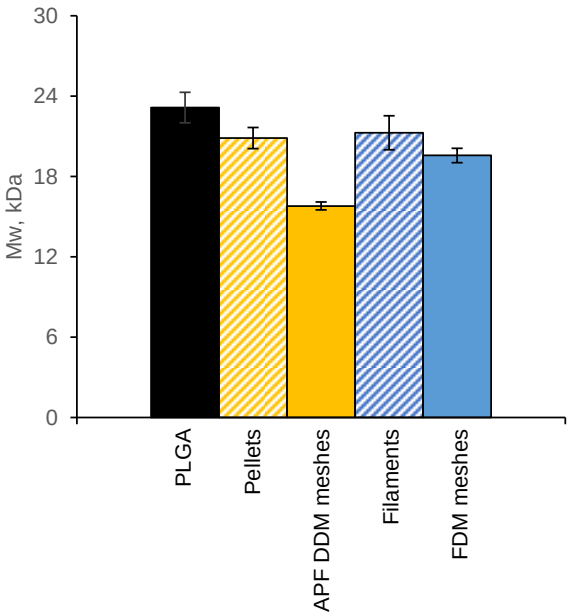

Fig 4: PLGA polymer molecular weight (Mw, determined by GPC) of the raw material, hot melt extruded pellets, implants prepared by APF DDM, hot melt extruded filaments and implants prepared by FDM.

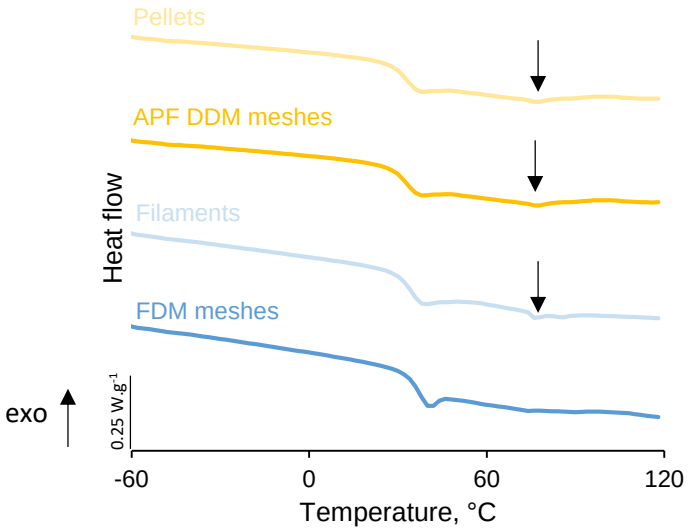

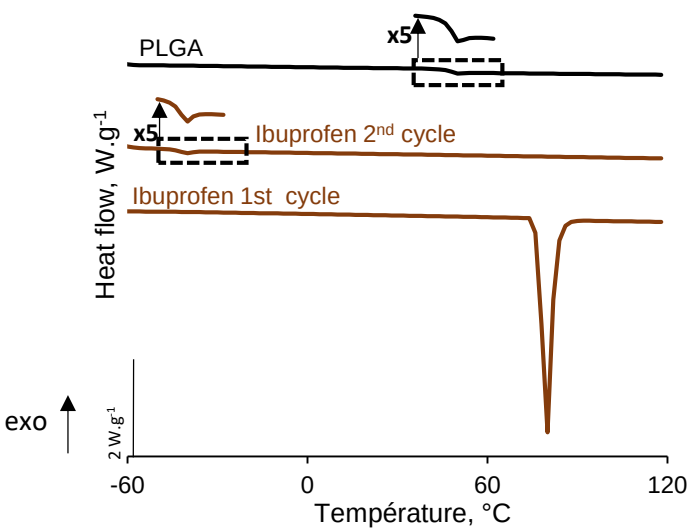

Fig 5: DSC thermograms of ibuprofen-loaded PLGA pellets, implants prepared by APF DDM, filaments and implants prepared by FDM (1^{st} heating cycles). For reasons of comparison, also the thermograms of PLGA raw material (2^{nd} heating cycle) and ibuprofen raw material (1^{st} and 2^{nd} heating cycle) are shown. The black flashes highlight the melting of crystalline ibuprofen.

3.3. In vitro drug release kinetics

Figure 6 shows the observed in vitro drug release kinetics in phosphate buffer pH 7.4 from the investigated APF DDM and FDM printed implants. In Figure 6A, the *relative* cumulative amounts of drug release are plotted, in Figure 6B the respective *absolute* amounts. Clearly, a major impact of the 3D printing technique on the resulting drug release patterns is observed, in particular:

- Drug release was complete after only about 1 week from FDM printed implants, whereas APF DDM printed meshes released ibuprofen during approximately 2 weeks.
- Ibuprofen release from FDM printed implants seemed to be mono-phasic, while 3 release phases could be distinguished from APF DDM printed meshes: an initial burst phase (during the 1st day), followed by an about constant drug release phase (from day 2 to day 4), and a final (again rapid) drug release phase, leading to complete ibuprofen exhaust.
- The absolute amount of ibuprofen released was much higher from APF DDM printed implants compared to FDM printed meshes: about 26.5 vs. 10.6 mg.

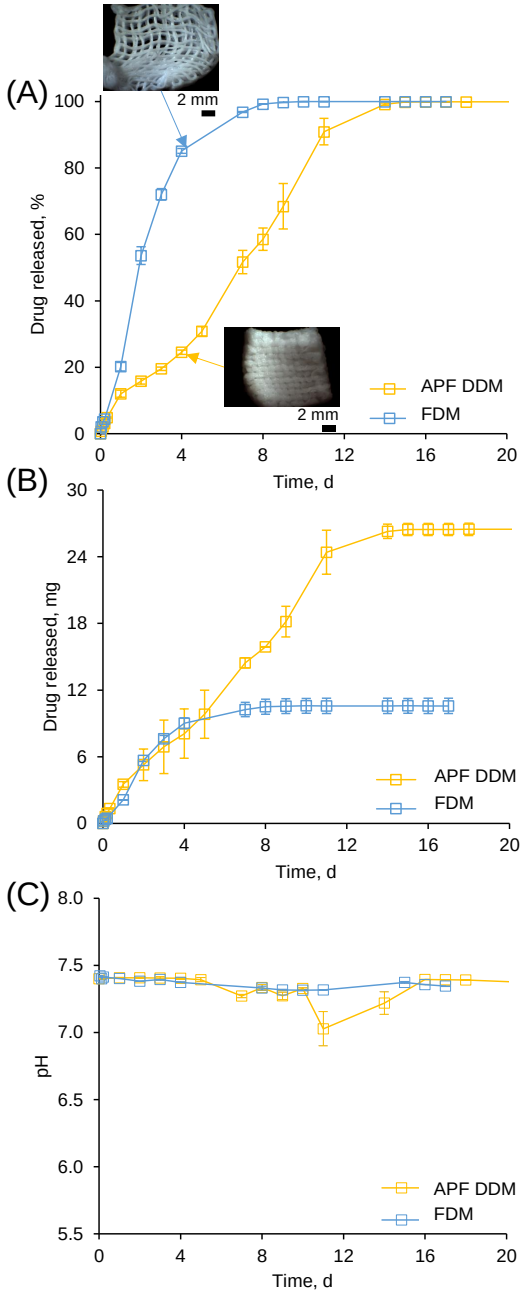

Fig 6: Ibuprofen release from PLGA implants prepared by Arburg Plastic Freeforming Droplet Deposition Modeling (APF DDM) or Fused Deposition Modeling (FDM) in phosphate buffer pH 7.4: (A) relative release rates, (B) absolute release rates, and (C) dynamic changes in the pH of the bulk fluid over time .

The difference in the total amounts of ibuprofen released at the end of the experiments can be explained by the different *real* filling densities of the implants (discussed above): Due to the *curved and thicker* filaments in APF DDM implants, the porosity of these meshes is much lower compared to FDM printed meshes, which are built of *straight and thinner* filaments. Since the outer dimensions of the implants were kept constant (10 x 10 x 2.5 mm), the weight of the APF DDM implants was higher (212 vs. 90 mg) and, thus, the amount of incorporated drug. To better understand the other marked differences in the drug release patterns and to get an idea of the underlying drug release mechanisms, dynamic changes in the systems' dry and wet mass, PLGA polymer molecular weight, inner and outer morphology as well as in the pH of the bulk fluid were monitored during drug release.

3.4. Drug release mechanism

The dynamic changes in the wet mass of the 3D printed PLGA implants upon exposure to the release medium are illustrated in Figure 7A: The blue and yellow curves correspond to FDM and APF DDM printed meshes, respectively. In both cases, substantial system swelling set on after about 4 d: the wet weight increased by more than 300 %. This fundamentally changed the conditions for drug release. The optical microscopy pictures in Figure 8 clearly illustrate the importance of this phenomenon for APF DDM printed implants after 7 d (top row) (FDM printed meshes became too fragile to be withdrawn from the bulk fluid without damage).

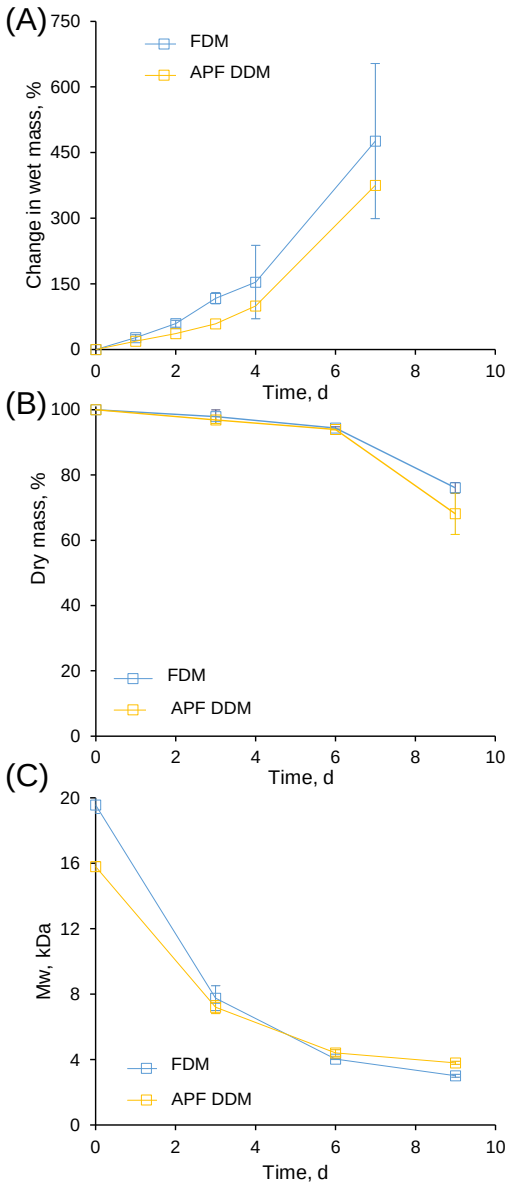

Fig 7: Dynamic changes in the: (A) wet mass (%), (B) dry mass (%), and (C) PLGA polymer molecular weight (Mw) of ibuprofen-loaded implants prepared by Arburg Plastic Freeforming Droplet Deposition Modeling (APF DDM) or Fused Deposition Modeling (FDM) upon exposure to phosphate buffer pH 7.4.

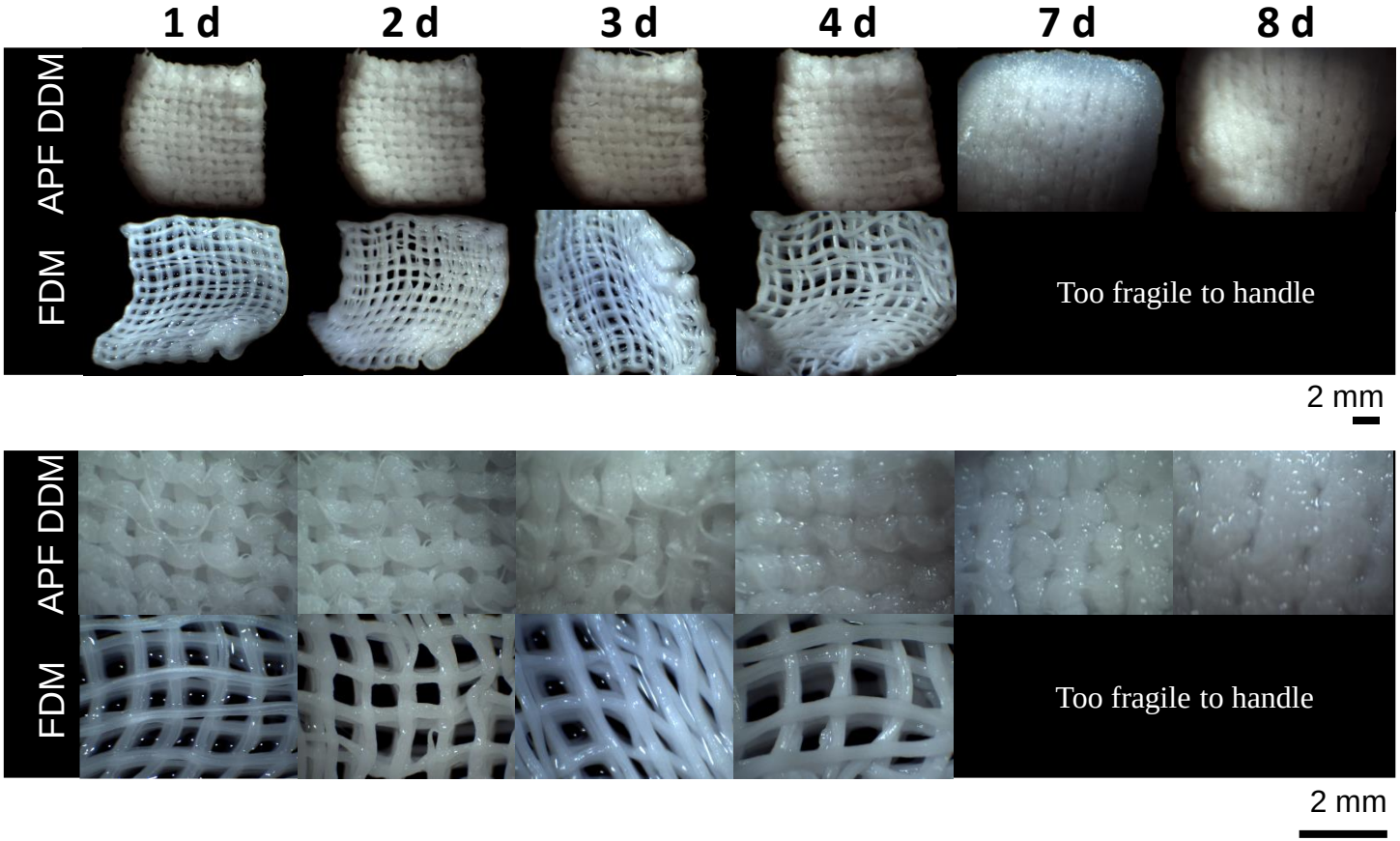

Fig 8: Optical macroscopy pictures of ibuprofen-loaded implants prepared by Arburg Plastic Freeforming Droplet Deposition Modeling (APF DDM) or Fused Deposition Modeling (FDM) upon different exposure periods to phosphate buffer pH 7.4 (indicated at the top). FDM printed implants became too fragile to be handled after 7 d exposure to the release medium.

The SEM pictures of surfaces (at the top of Figure 9) and cross sections (at the bottom of Figure 9) of implants after 3 d exposure to the release medium further evidence dynamic changes in the inner implant structure. Please note that the samples had to be dried before SEM analysis, so great caution must be paid: during drying artefacts have been created. As it can be seen, the surfaces of all samples became highly wizened. This does not represent the real surface structures of the implants during drug release: The high water concentrations at the implants' surfaces lead to significant PLGA swelling in these outer regions. Thus, during drug release, the surfaces consist of highly swollen polymer gels (as it can be seen in Figure 8). Upon drying, the wizened structure is artificially created. The inner structure of the PLGA filaments becomes more and more porous with time. For instance, comparing the SEM pictures of cross sections before and after 3 d exposure to the release medium (Figure 3 vs. 9), much larger pores can be seen. This is due to polymer degradation occurring throughout the system.

Figure 7B shows that the dry mass of the 3D printed implants only slightly decreased during the first week, and then significantly dropped. The dynamic changes in the PLGA polymer molecular weight are illustrated in Figure 7C: Interestingly, the initial differences in Mw for APF DDM and FDM printed implants (about 20 vs. 16 kDa, discussed above) vanished after a few days. Furthermore, the pH of the release medium stayed about constant during the entire observation period in the case of FDM printed implants (Figure 6C), whereas in the case of the APF DDM printed meshes, a temporary (limited) drop in pH was observed after about 12 d.

It has to be pointed out that the *absolute* cumulative amounts of ibuprofen released from APF DDM and FDM printed implants were rather similar during the first 4 d (Figure 6B). This can at least in part be explained by the fact that the ibuprofen-PLGA filaments were not substantially different in composition and inner & outer structure. Once the meshes get into contact with the release medium, water penetrates into the system and rather rapidly wets the entire PLGA matrix. Most of the drug is already dissolved (in the form of individual molecules/ions) in the polymer (only minor amounts of ibuprofen crystals need to dissolve in the case of APF DDM printed implants). The presence of the water in the polymeric network increases the mobility of the drug molecules/ions. Due to concentration gradients the latter diffuse out of the system. The conditions for water penetration and drug diffusion are rather similar for APF DDM and FDM printed implants, hence, the resulting *absolute* drug release rates are similar. Also, the higher implant mass in the case of APF DDM printed meshes can be expected to be at least partially be compensated by a higher surface area accessible for drug release in the case of FDM printed meshes.

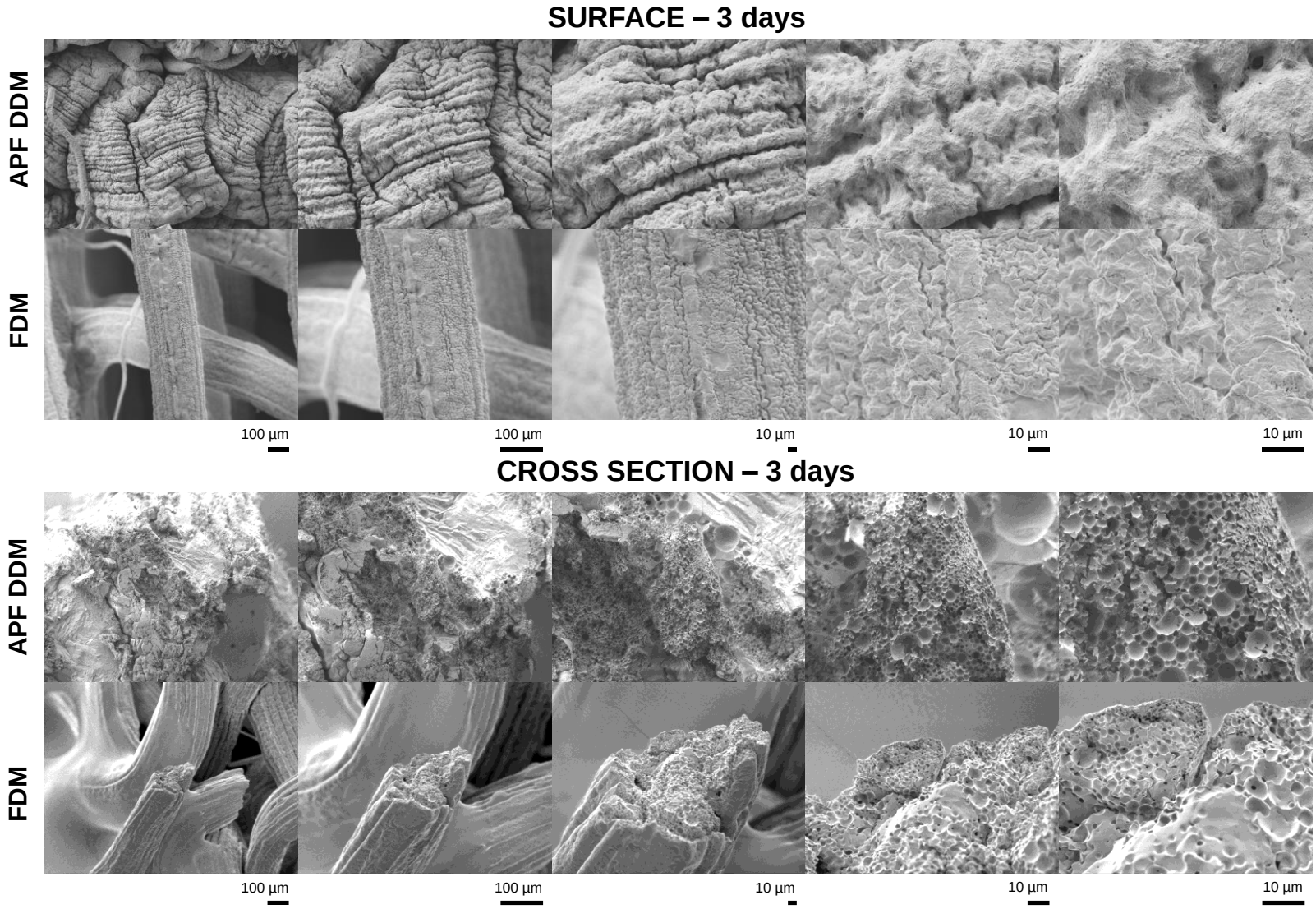

Fig 9 SEM pictures of surfaces and cross sections of ibuprofen-loaded PLGA implants prepared by Arburg Plastic Freeforming Droplet Deposition Modeling (APF DDM) or Fused Deposition Modeling (FDM) after 3 d exposure to phosphate buffer pH 7.4. Please note that the samples were freeze-dried prior to analysis. Thus, caution must be paid due to artefact creation.

Importantly, more than 85 % of the ibuprofen were released after only about 4 d from FDM printed implants, while most of the drug was still entrapped in the APF DDM printed implants at this time point. This is due to the different *real* filling density of the meshes: As it can be seen in Figure 8, all filaments are surrounded by well agitated release medium in the case of FDM printed implants. Once a drug molecule/ion is released from a PLGA filament, *convective* mass transport through the large pores of the meshes guarantees rapid distribution throughout the entire bulk fluid. Thus, the longest *diffusion* pathway to be overcome for an ibuprofen molecule/ion, in order to be released, is the radius of a PLGA filament (in the "worst" case, the drug is located right at the center of the filament). For this diffusional mass transport step, about 4 d are required. In contrast, if a drug molecule/ion is released from a PLGA filament located in an implant which was printed by FDM, it is not further transported by a convective bulk fluid flow. Instead, the drug has to diffuse through a continuous PLGA gel (e.g., Figure 8, top row, photo after 7 d) before reaching the agitated bulk fluid. This is because the porosity of the APF DDM printed meshes was much lower than the porosity of FDM printed implants and PLGA swelling closed the water-filled pores. Thus, the drug has to diffuse through a more or less dense PLGA "gel", which is created by the fusion of highly swollen (initially individual) polymer filaments. The diffusion pathways to be overcome in this gel are much longer compared to those in a single filament. Consequently, drug release is slowed down.

If diffusion through this gel was the only dominant drug release mechanism, the resulting release rate would be expected to decrease with time (due to the decreasing drug concentration gradients). However, after about 4 d, the opposite was observed: A final rapid drug release phase started from APF DDM printed implants. This can be explained as follows: After about 4 d, substantial PLGA swelling set on (Figure 7A and 8). For FDM printed implants, this did not affect drug release, because most of ibuprofen was already released at this time point. However, in the case of APF DDM printed implants, this substantial polymer swelling lead to an increase in the mobility of the drug molecules/ions, which were still entrapped: The distance between the polymer chains became larger, and the mobility of the macromolecules increased. Consequently, the drug molecules/ions could more easily move within the (now highly swollen) PLGA network. The possible root cause for this substantial PLGA swelling, which can often be observed after a certain lag phase, has previously been described in more detail [49]. In brief, the PLGA matrix is initially rather hydrophobic, limiting the amounts of water penetrating into the system. Nevertheless, the entire PLGA matrix is rather rapidly wetted (by limited amounts of water) and polymer hydrolysis occurs throughout the system ("bulk erosion"). Importantly, upon hydrolysis of an ester bond, two new *hydrophilic* end groups are created: a -COOH group and a -OH group. Hence, the polymer matrix becomes more and more hydrophilic with time, facilitating further water penetration into the system. In addition, the polymer chains become shorter and, thus, less entangled, offering less mechanical hindrance to the penetration of high amounts of water into the polymer matrix. Furthermore, water-soluble, short chain degradation products are created inside the system, generating a continuously increasing osmotic pressure attracting water. All these phenomena lead to substantial system swelling of PLGA-based matrices after a certain lag time.

Once substantial implant swelling sets on, not only the mobility of ibuprofen, but also the mobility of water-soluble PLGA degradation products (short chain acids) increases. Due to concentration gradients, these water-soluble acids are released into the surrounding bulk fluid. The release of both: "ibuprofen and polymer degradation products" cause the onset of important dry mass loss after about 1 week (Figure 7B). The observed temporary drop in the pH of the release medium during the "week-end sampling pause" after about 9 d in the case of APF DDM printed implants (Figure 6C) can likely be attributed to the fact that the sampling pause coincides with the final rapid ibuprofen and short chain acid release phase from these implants (Figure 8A). The absence of such a drop in the case of FDM printed implants can probably be

explained by the fact that most of ibuprofen had already been released before, and that the mass of the mesh is much lower (90 vs. 212 mg), thus, the absolute amounts of generated short chain acids was much lower.

Another reason for the observed faster ibuprofen release from the FDM printed implants compared to APF DDM printed meshes is the increase in total implant size upon exposure to phosphate buffer pH 7.4: As it can be seen in Figure 8, already after 1 d the FDM printed mesh covered a larger area than the APF DDM printed mesh. This can at least in part be attributed to the lower mechanical stability of the more porous mesh consisting of thinner PLGA filaments in the case of FDM printed implants.

4. Conclusion

Both 3D printing techniques: "APF DDM and FDM" can be used to prepare controlled release PLGA implants. However, since individual droplets are deposited during APF DDM, and not continuous filaments, the resulting geometry of the implants can differ, even if using the same composition and identical (theoretical) device design. These structural differences can lead to altered conditions for drug release, e.g. differences in the mesh porosity and, hence, different release kinetics of the drug. Please note that the importance of these effects depends on the specific implant design and processing conditions. The properties of the obtained implants should be fine-tuned to match the needs for each application, e.g. with respect to the resulting drug release kinetics and mechanical properties. It has to be pointed out that the *real* filling density/porosity of 3D printed PLGA implants is of key importance for the release patterns, determining the mobility of the drug in the polymeric system.

Acknowledgements

This project has received funding from the Interreg 2 Seas programme 2014-2020 co-funded by the European Regional Development Fund under subsidy contract No 2S04-014 3DMed. The authors are very grateful for this support. They would also like to thank Mr. A. Fadel from the "Centre Commun de Microscopie" of the University of Lille ("Plateau techique de la Federation Chevreul CNRS FR 2638") for his valuable technical help with the SEM pictures.

References

1 Park H, Otte A, Park K. Evolution of drug delivery systems: From 1950 to 2020 and beyond. J Control Release 342 (2022) 53-65.

2 Wan F, Yang M. Design of PLGA-based depot delivery systems for biopharmaceuticals prepared by spray drying. Int J Pharm 498 (2016) 82–95.

3 Park K, Skidmore S, Hadar J et al. Injectable, long-acting PLGA formulations: Analyzing PLGA and understanding microparticle formation J Control Release 304 (2019) 125-134.

4 Permana AP, Mir M, Utomo E et al. Bacterially sensitive nanoparticle-based dissolving microneedles of doxycycline for enhanced treatment of bacterial biofilm skin infection: A proof of concept study Int J Pharmaceut X 2 (2020) 100047.

5 Chen W, Palazzo A, Hennink WE et al. Effect of Particle Size on Drug Loading and Release Kinetics of Gefitinib-Loaded PLGA Microspheres. Mol Pharm 14 (2017) 459–67.

6 Wang J, Wang BM, Schwendeman SP. Characterization of the initial burst release of a model peptide from poly(D,L-lactide-co-glycolide) microspheres. J Control Release 82 (2002) 289–307.

7 Anderson J, Shives M. Biodegradation and biocompatibility of PLA and PLGA microspheres. Adv Drug Deliv Rev 28 (1997) 5–24.

8 Lehner E, Guendel D, Maeder K. Intracochlear PLGA based implants for dexamethasone release: Challenges and solutions. Int J Pharmaceut X 1 (2019) 100015.

9 Bassand C, Freitag J, Benabed L, Verin J, Siepmann F, Siepmann J. PLGA implants for controlled drug release: Impact of the diameter. Eur J Pharm Biopharm 177 (2022) 50-60.

10 Cosse A, Koenig C, Lamprecht A et al. Hot Melt Extrusion for Sustained Protein Release: Matrix Erosion and In Vitro Release of PLGA-Based Implants. AAPS Pharm Sci Tech 18 (2017) 15-26.

11 Maturavongsadit P, Paravyan G, Kovarova M et al. A new engineering process of biodegradable polymeric solid implants for ultra-long-acting drug delivery. Int J Pharmaceut X 3 (2021) 100068.

12 Lehner A, Liebau K, Syrowatka et al. Novel biodegradable Round Window Disks for inner ear delivery of dexamethasone. Int J Pharmaceut 594 (2020) 120180.

13 Kempe S, Metz H, Maeder K. Do in situ forming PLG/NMP implants behave similar in vitro and in vivo? A non-invasive and quantitative EPR investigation on the mechanisms of the implant formation process. J Control Release 130 (2008) 220-225.

14 Lin S, Cui L, Chen G et al. PLGA/β-TCP composite scaffold incorporating salvianolic acid B promotes bone fusion by angiogenesis and osteogenesis in a rat spinal fusion model. Biomaterials 196 (2019) 109-121.

15 Serris I, Serris P, Frey KM et al. Development of 3D-Printed Layered PLGA Films for Drug Delivery and Evaluation of Drug Release Behaviors. AAPS Pharm Sci Tech. 21 (2020) https://doi.org/10.1208/s12249-020-01790-1.

16 Goole J, Amighi K. 3D printing in pharmaceutics: A new tool for designing customized drug delivery systems. Int J Pharmaceut. 499 (2016) 376-394.

17 Bom S, Martins AM, Ribeiro HM et al. Diving into 3D (bio)printing: A revolutionary tool to customize the production of drug and cell-based systems for skin delivery Int J Pharmaceut. 605 (2021) 120794.

18 Wang J, Zhang Y, Aghda NH et al. Emerging 3D printing technologies for drug delivery devices: Current status and future perspective. Adv Drug Deliv Rev. 174 (2021) 294-316.

19 Parhi, R. A review of three-dimensional printing for pharmaceutical applications: Quality control, risk assessment and future perspectives. J Drug Del Sci Tech 64 (2021) 102571.

20 Maroni A, Melocchi A, Parietti F et al. 3D printed multi-compartment capsular devices for two-pulse oral drug delivery. J Controld Release 268 (2017) 10-18.

21 Ragelle H, Rahimian S, Guzzi EA et al. Additive manufacturing in drug delivery: Innovative drug product design and opportunities for industrial application. Adv Drug Deliv Rev. 178 (2021) 113990.

22 Sharifi M, Bai Q, Babadaei MMN et al. 3D bioprinting of engineered breast cancer constructs for personalized and targeted cancer therapy. J Control Release 333 (2021) 91-106.

23 Seoane-Viano I, Januskaite P, Alvarez Lorenzo C et al. Semi-solid extrusion 3D printing in drug delivery and biomedicine: Personalised solutions for healthcare challenges. J Control Release 332 (2021) 367-389.

24 Elkasabgy NA, Mahmoud AA, Maged A. 3D printing: An appealing route for customized drug delivery systems. Int J Pharmaceut. 588 (2020) 119732.

25 Reddy RDP, Sharma V. Additive manufacturing in drug delivery applications: A review. Int J Pharmaceut 589 (2020) 119820.

26 Martinez PR, Goyanes A, Basit AW et al. Fabrication of drug-loaded hydrogels with stereolithographic 3D printing. Int J Pharm. 532 (2017) 313-317.

27 Goyanes A, Robles Martinez P, Buanz A et al. Effect of geometry on drug release from 3D printed tablets. Int J Pharm. 494 (2015) 657-663.

28 Muwaffak Z, Goyanes A, Clark V et al. Patient-specific 3D scanned and 3D printed antimicrobial polycaprolactone wound dressings. Int J Pharm. 527 (2017) 161-170.

29 McDonagh T, Belton P, Qi, S. Direct Granule Feeding of Thermal Droplet Deposition 3D Printing of Porous Pharmaceutical Solid Dosage Forms Free of Plasticisers. Pharm Res 39 (2022) 599–610.

30 Goyanes A, Allahham N, Trenfield SJ et al. Direct powder extrusion 3D printing: Fabrication of drug products using a novel single-step process. Int J Pharm. 567 (2019) 118471.

31 Awad A, Fina F, Goyanes A et al. Advances in powder bed fusion 3D printing in drug delivery and healthcare. Adv Drug Deliv Rev. 174 (2021) 406-424.

32 Fina F, Goyanes A, Gaisford S et al. Selective laser sintering (SLS) 3D printing of medicines. Int J Pharm. 529 (2017) 285-293.

33 Carlier E, Marquette S, Peerboom C et al. Development of mAb-loaded 3D-printed (FDM) implantable devices based on PLGA. Int J. Pharmaceut. 597 (2021) 120337.

34 Manini G, Benali, S, Mathew A et al. Paliperidone palmitate as model of heat-sensitive drug for long-acting 3D printing application. Int J Pharmaceut. 618 (2022) 121662.

35 Chou PY, Lee D, Chen SH et al. 3D-printed/electrospun bioresorbable nanofibrous drug-eluting cuboid frames for repair of alveolar bone defects. Int J Pharmaceut. 615 (2022) 121497.

36 Kraibuhler H, Duffner E. Device for the production of a three-dimensional object. US20140113017A1 (2018) 9889604.

37 Kraibuhler H, Duffner E, Kessling O. Method for producing a three-dimensional object by means of generative construction. Patent 20160009026 (2018) 10040249.

38 Welsh NR, Malcolm RK, Devlin B et al. Dapivirine-releasing vaginal rings produced by plastic freeforming additive manufacturing. Int J Pharm. 572 (2019) 118725.

39 Fredenberg S, Wahlgren M, Reslow M et al. The mechanisms of drug release in poly(lactic-co-glycolic acid)-based drug delivery systems--a review. Int J Pharmaceut. 415 (2011) 34–52.

40 Fredenberg S, Joensson M, Laakso T et al. Development of mass transport resistance in poly(lactide-co-glycolide) films and particles – A mechanistic study. Int J Pharmaceut. 409 (2011) 194–202.

41 Goepferich, A. Mechanisms of polymer degradation and erosion. Biomaterials 17 (1996) 103–114.
42 Huang, J, Mazzara, JM, Schwendeman, SP et al. Self-healing of pores in PLGAs. J Control Release. 206 (2015) 20–29.
43 Fu, K, Pack, DW, Klibanov, AM et al. Visual Evidence of Acidic Environment Within Degrading Poly(lactic-co-glycolic acid) (PLGA) Microspheres. Pharm Res. 17 (2000) 100–106.
44 Schaedlich, A, Kempe, S, Maeder K. Non-invasive in vivo characterization of microclimate pH inside in situ forming PLGA implants using multispectral fluorescence imaging. J Control Release 179 (2014) 52-62.
45 Brunner, A, Maeder K, Goepferich, A. pH and osmotic pressure inside biodegradable microspheres during erosion. Pharm Res. 16 (1999) 847–853.
46 Blasi P, Schoubben A, Giovagnoli S et al. Ketoprofen poly(lactide-co-glycolide) physical interaction. AAPS Pharm Sci Tech. 8 (2007) E78–E85.
47 Blasi P, D'Souza SS, Selmin F et al. Plasticizing effect of water on poly(lactide-co-glycolide). J Control Release. 108 (2005) 1–9.
48 Tamani F, Bassand C, Hamoudi M et al. Mechanistic explanation of the (up to) 3 release phases of PLGA microparticles: Diprophylline dispersions. Int J Pharmaceut. 572 (2019) 118819.
49 Bode C, Kranz H, Fivez A et al. Often neglected: PLGA/PLA swelling orchestrates drug release - HME implants. J Control Release 306 (2019) 97-107.
50 Kozak J, Rabiskova M, Lamprecht A. In-vitro drug release testing of parenteral formulations via an agarose gel envelope to closer mimic tissue firmness. Int J Pharmaceut. 594 (2021) 120142.
51 Bassand C, Verin J, Lamatsch M et al. How agarose gels surrounding PLGA implants limit swelling and slow down drug release. J Control Release 343 (2022) 255-266.
52 Bassand C, Benabed L, Verin J et al. Hot melt extruded PLGA implants loaded with ibuprofen: How heat exposure alters the physical drug state. J Drug Dev Sci Tech 73 (2022) 103432.